EUROPEAN ORGANIZATION FOR NUCLEAR RESEARCH

CERN-EP/86-201
28.11.1986

ON THE HYPERFINE STRUCTURE AND ISOTOPE SHIFT OF RADIUM

K. Wendt, S.A. Ahmad[1], W. Klempt,
R. Neugart, E.W. Otten, H.H. Stroke[2]

The ISOLDE Collaboration, CERN, Geneva, Switzerland
and
Institut für Physik, Universität Mainz, Mainz,
Fed. Rep. of Germany

Abstract

The hyperfine structure and isotope shift of the heaviest known alkaline earth element radium (Z = 88) have been studied in both the atomic Ra I and ionic Ra II spectra. The measurements, carried out by on-line collinear fast-beam laser spectroscopy, yield the hyperfine constants A and B of the 7s and $7p_{1/2}$ states in Ra II, of all states of the excited 7s7p configuration and the 7s7d $^3D_3$ state in Ra I. The data allow a consistent evaluation of the nuclear moments for eight odd-A radium isotopes. In particular, a complete analysis of the hyperfine structure of the sp configuration in the two-electron system provides a stringent test of the validity of the semi-empirical modified Breit-Wills theory. It is shown that the effective operator formalism is equivalent, if relativistic correction functions are used to reduce the number of parameters. The semi-empirical hyperfine fields are evaluated and found to agree generally with those from ab-initio calculations. The isotope shifts in the s-p, s^2-sp, sp-sd transitions are analysed semi-empirically and compared with ab-initio calculations. The consistency of the different analyses proves their validity and classifies the spectrum of Ra I as a model case for a simple and clean two-electron spectrum.

[1]On leave from: Bhabha Atomic Research Centre, Bombay, India
[2]On leave from: New York University, New York, USA

1. INTRODUCTION

Radium is the only alkaline earth element of which optical hyperfine structures (hfs) and isotope shifts (IS) remained unknown until very recently [1]. Previous atomic spectroscopic studies concerning the level structure of Ra I and Ra II were performed only on the long-lived, doubly-even isotope ^{226}Ra ($T_{1/2}$ = 1600 a) [2,3]. The evaluation of nuclear dipole and electric quadrupole moments from the measured hyperfine interaction constants A and B requires the knowledge of the hyperfine fields at the nucleus. Similarly, the IS are related to the isotopic changes in the nuclear mean square charge radii via the electron densities of the states involved in the optical transitions. The basis for an analysis of the hfs and IS can be provided by systematic investigations in a number of states of both the neutral atom (Ra I) and the alkali-like singly-charged ion (Ra II). A coherent description of the hfs and IS also provides a test for semi-empirical models and ab-initio theories. For the heavy element radium (Z = 88) they are particularly sensitive to relativistic contributions and the finite nuclear size effect. From the nuclear physics point of view there is a special interest in the moments and charge radii of radium, as experimental and theoretical evidence for the occurence of reflection asymmetric nuclear shapes [4,5] has been found in the region $86 \leq Z \leq 90$ and $130 \leq N \leq 140$.

We have measured the hfs in four levels of Ra I and two levels of Ra II, connected by the four transitions shown in the level schemes of Fig. 1 a) and b). In Ra I the experiments yielded a complete set of hfs parameters of the first excited 7s7p configuration and those of the 7s7d $^3D_3$ state. The $^1P_1$ and $^3P_1$ states were excited from the $^1S_0$ ground state by the strong resonance line at 4826 Å and the weaker intercombination line at 7141 Å, respectively. The metastable $^3P_2$ and the $^3D_3$ state were investigated in the 6446 Å transition. In the alkali-like one-electron spectrum of Ra II only the "D_1 line" 7s $^2S_{1/2}$ - 7p $^2P_{1/2}$ at 4683 Å was studied, while the ultraviolet "D_2 line" to the 7p $^2P_{3/2}$ state at 3814 Å could not been reached so far.

The measurements include the hfs of 8 odd-A isotopes, and the IS of altogether 19 isotopes in the mass range $208 \leq A \leq 232$.

The experiment has been performed by on-line collinear fast-beam laser spectroscopy, which combines the features of high sensitivity (required for the study of short-lived isotopes with low production yield) and high resolution (required for the investigation of hfs and IS with high precision). In discussing the results, this paper will focus on the atomic physics aspect, in particular on the consistent description of the hfs in the two-electron 7s7p configuration in Ra I. Here, the modified Breit-Wills theory (MBWT) [6,7] and also the effective operator formalism (EOF) [8] have been applied. This parallel treatment has been chosen for a couple of reasons:

i) The semi-empirical approach of the MBWT gives an adequate description of the two-electron hfs in all known alkaline-earth spectra including the subgroup II elements. This is due to an effective inclusion of configuration interactions. The validity of this approach in a strongly relativistic case is shown by the comparison of the emerging nuclear dipole moments with those obtained from the alkali-like Ra II spectrum.

ii) The effective operator approach in its original formulation [8] is a correct parametrisation of the hfs (including relativistic corrections and core polarization), as long as configuration interactions are neglected. In particular, it neglects the fact, that the radial wave functions within one configuration differ considerably from one multiplet to the other, due to the exchange interaction. The attempt of generalizing the effective operator formalism by the assumption of different interaction constants for each multiplet, increases the number of parameters. In the sp configurations they exceed by far the number of input parameters available from the experiment. Thus the application to radium involves certain simplifications. Nevertheless, together with the interaction parameters from recent ab-initio calculations, it gives new insight into the hfs of Ra I and elucidates the relativistic corrections entering into the semi-empirical approach.

The semi-empirical mixing coefficients, hfs fields and electronic field shift factors which are essential for a quantitative determination of nuclear moments and radii are compared with ab-initio values [9,10,11,12]. The agreement is satisfying and supporting both approaches.

In section 2 we give a brief description of the experimental set-up and the extraction of the data from the optical spectra. Sections 3 and 4 deal with the MBWT and the EOF analyses. Section 5 treats the hfs fields and section 6 the electronic field shift factors and specific mass shifts.

A first interpretation of spins and moments within nuclear models has been given already in [1]. It will be resumed in a forthcoming paper [13], together with an extensive discussion of the isotope shift of nuclear mean square charge radii and their relationship to nuclear deformation. There the discussion will focus on the possible existence of a stable octupole deformation (see also [14]).

2. EXPERIMENT AND RESULTS

The experiment has been performed using the set-up for collinear fast-beam laser spectroscopy [15] which is installed on line with the mass separator facility ISOLDE at CERN [16]. ISOLDE gives high yields of radium isotopes, from proton-induced spallation of ^{238}U. The 600-MeV beam from the CERN synchro-cyclotron is hitting a UC_2 cloth target (12 g/cm^2) which is heated to 2200° C to release the volatile spallation products. The evaporated atoms are ionized on a hot tungsten surface (2400° C) and extracted in the form of a 60-keV ion beam. After mass separation this beam is bent into the axis of the laser beam and transmitted through the set-up for charge-exchange neutralization and fluorescence detection. With a kinetic energy spread of about 2 eV the total absorption line width is about 30 MHz. This is of the order of the natural line width of the strong transitions $^2S_{1/2} - {}^2P_{1/2}$, $^1S_0 - {}^1P_1$ and $^3P_2 - {}^3D_3$. The natural width of the weak intercombination line $^1S_0 - {}^3P_1$ can be estimated from the singlet-triplet mixing coefficients to be about 500 kHz. Power broadening is

used to cover the Doppler profile by the homogeneous line width, which gives the maximum fluorescence signal. Experimental details on the collinear fast-beam laser spectroscopy on neutral atoms are given in [15,17]. The metastable $7s7p\ ^3P_2$ level is populated in the near-resonant charge-exchange process by using cesium instead of sodium vapour as exchange partner (compare Fig. 1b). This procedure was first applied in the study of radioactive Yb isotopes [18]. A slight modification of the set-up for studying the ionic resonance lines was used already for investigations in the Ba II spectrum [19]. The charge-exchange cell is removed and the observation region is electrically insulated to form a Faraday cage for the application of the post-acceleration/deceleration voltage.

The light source was a commercial frequency-stabilized cw dye laser with the dyes Coumarin 102 (4683 Å, 4826 Å), Rhodamin 101 (6446 Å) and Oxazine 1 (7141 Å), pumped by an argon or krypton ion laser. The dye laser is running at fixed frequency while the frequency tuning in the rest frame of the fast moving atoms is performed by a change of the ion energy. With a post-acceleration/deceleration of ± 10 keV, the Doppler-tuning range amounts to ± 30 GHz at 7141 Å and ± 40 GHz at 4683 Å. The optical resonances are observed by counting the fluorescence photons as a function of the post-acceleration voltage. Fluorescence signals could be observed down to isotopic yields of about 10^4 atoms/s. This sensitivity led to the discovery of the new isotope ^{232}Ra.

A typical hfs pattern in the 6446 Å line is shown in Fig. 2 for ^{221}Ra (I = 5/2). (Corresponding hfs patterns for ^{223}Ra in the 4683 Å and 4826 Å lines obtained with a much better signal-to-noise ratio are found in [1]). The hfs and the IS between two isotopes is obtained from the respective resonance voltages via the relativistic Doppler equation. For the odd-A isotopes a computer fit yields directly the A and B factors and the centers of gravity from the observed hfs patterns. The results are compiled in Tables 1 and 2.

A special problem arises for the hfs of the $^3D_3$ state which has to be corrected for second order hfs contributions due to the admixture of hfs components from a $^1D_2$ state lying only 17 cm^{-1} apart (compare Fig. 1b). This state has been assigned to the $7p^2$ configuration [3]. However, the hfs operator does not connect the 7s7d and $7p^2$ configurations. Therefore, we assume the perturbing state to belong predominantly to 7s7d. Second-order perturbation theory gives a contribution to the $^3D_3$ hfs via the reduced off-diagonal matrix element $\langle 7s7d\ ^3D_3 || \mathcal{H}^{(1)}_{hfs} || 7s7d\ ^1D_2 \rangle$ for which a fit of the disturbed experimental hfs yields 156(12) MHz, while the theoretical estimate $\langle 7s7d\ ^3D_3 || \mathcal{H}^{(1)}_{hfs} || 7s7d\ ^1D_2 \rangle \approx \frac{1}{12} c_1' a(7s)$ [20] (with a(7s) taken from Table 3) gives 172(10) MHz. This good agreement supports the assignment 7s7d to the $^1D_2$ state at 32215 cm^{-1}. The hfs parameters of $^3D_3$ in Table 2 are corrected for this effect.

The errors quoted in Tables 1 and 2 are the sum of systematic errors, mainly due to $1 \cdot 10^{-4}$ uncertainties in the acceleration and post-acceleration voltages, and an one standard deviation error from the fitting routine. Both uncertainties are of the same order and yield the total experimental errors of about 1 - 10 MHz. A plot of the measured IS values in the Ra II 4683 Å line, relative to the isotope ^{214}Ra, is given in Fig. 3 which also shows the hfs of the odd-A isotopes. The corresponding figure for the Ra I 4826 Å line can be found in [1].

3. ANALYSIS OF HFS WITH THE MODIFIED BREIT-WILLS THEORY

3.1 General Presentation

Breit and Wills developed a general formalism to decompose the hfs parameters A_J, B_J of a pure two-electron configuration with intermediate coupling into the contributions of the individual electrons $a_{n\ell j}$, $b_{n\ell j}$ [21]. In central field approximation the latter ones are given [22] by

$$a_{ns} = (8\pi/3)\ (2\mu_o\mu_B/4\pi)\ (\mu_I/I)\ |\Psi(0)|^2_{ns}\ F_{1/2}(Z_i)\ (1-\delta)\ (1-\varepsilon) \qquad (1)$$

$$a_{n\ell j} = (2\mu_o\mu_B/4\pi)\ (\mu_I/I)\ \{\ell(\ell+1)/j(j+1)\}\ \langle r^{-3}\rangle_{n\ell}\ F_j(Z_i)\ (1-\delta)\ (1-\varepsilon) \quad (2)$$

$$b_{n\ell j} = (e^2/4\pi\varepsilon_o)\ Q_s\ [(2j-1)/(2j+2)]\ \langle r^{-3}\rangle_{n\ell}\ R_{\ell j}(Z_i) \quad (3)$$

The hyperfine fields arise from the (non-relativistic) electron density $|\psi(0)|^2_{ns}$ at the origin for an electron with $\ell = 0$ (contact term) and from the radial integral $\langle r^{-3}\rangle_{n\ell}$ for an electron with angular momentum $\ell > 0$. Equation (2) comprises the orbital and spin-dipole contributions to the hfs field without taking into account the contact term which is produced by the spin polarization of the core (compare section 4). Core polarization effects are also omitted in (1) and (3). $F_j(Z_i)$ and $R_{\ell j}(Z_i)$ are relativistic correction functions which take into account mainly the relativistic enhancement of the electronic wave function close to the origin. They were first given by Casimir [22,23] and later improved by Schwartz [24]. The relativistic Breit-Rosenthal-Schawlow correction $(1-\delta)$ describes the flattening of the Dirac wave function in the parabolic Coulomb potential inside the nucleus, while the Bohr-Weisskopf correction $(1-\varepsilon)$ takes into account the spatial distribution of the nuclear magnetization. By use of the well-known semi-empirical Goudsmit-Fermi-Segré formula, the electronic matrix elements can be related to known spectroscopic quantities [22] by

$$|\psi(0)|^2_{ns} = \frac{Z_i Z_o^2}{\pi a_o^3 n^{*3}}\ \left(1 - \frac{d\sigma}{dn}\right) \quad (4)$$

$$\langle r^{-3}\rangle^{FGS}_{n\ell} = Z_i Z_o^2/\{a_o^3 n^{*3} \ell(\ell+\tfrac{1}{2})\ (\ell+1)\} \quad (5)$$

with the effective charges Z_i and Z_o, the effective quantum number $n^* = n-\sigma$ and the quantum defect σ. For $\ell > 0$, $\langle r^{-3}\rangle_{n\ell}$ can be alternatively related to the fine structure splitting $\delta\nu_{fs}$ by

$$\langle r^{-3}\rangle^{(fs)}_{n} = \delta\nu_{fs}/\{a_o^3\ R_\infty\alpha^2(\ell+\tfrac{1}{2})\ Z_i H_r(\ell,Z_i)\} \quad (6)$$

$H_r(\ell,Z_i)$ is another relativistic correction.

The intermediate coupling is described either in terms of pure LS wave functions $|^{\beta,1}L_L\rangle_{LS}$ or pure jj wave functions $|s_{1/2},\ell_j\rangle$ by

$$|^3L_L\rangle = \alpha\,|^3L_L\rangle_{LS} + \beta\,|^1L_L\rangle_{LS}$$

$$= c_1\,|s_{1/2}, \ell_{\ell+1/2}\rangle + c_2\,|s_{1/2}, \ell_{\ell-1/2}\rangle \qquad (7a)$$

$$|^1L_L\rangle = -\beta\,|^3L_L\rangle_{LS} + \alpha\,|^1L_\ell\rangle_{LS}$$

$$= c_2\,|s_{1/2}, \ell_{\ell+1/2}\rangle - c_1\,|s_{1/2}, \ell_{\ell-1/2}\rangle \qquad (7b)$$

with normalized mixing coefficients α, β and c_1, c_2, respectively, which are interrelated by

$$\alpha = \sqrt{\frac{\ell}{2\ell+1}}\,c_1 + \sqrt{\frac{\ell+1}{2\ell+1}}\,c_2, \quad \beta = \sqrt{\frac{\ell+1}{2\ell+1}}\,c_1 - \sqrt{\frac{\ell}{2\ell+1}}\,c_2 \qquad (7c)$$

With the representation (7) the A_J and B_J factors can be expressed in terms of the single electron hfs constants (1-3) [21].

The modification of the original Breit-Wills theory consists in the allowance for different radial wave functions in the singlet and triplet states. These are produced by the strong Coulomb exchange interaction between the two valence electrons. In a region close to the nucleus ($r \lesssim 3a_0/Z$), where the hfs and fs interactions are strongest, the simple assumption of a proportionality between the radial wave functions in triplet and singlet states is justified [25]. The reason is that the shape of the wave function in this region is determined by the strong nuclear Coulomb field and the exchange interaction only affects its amplitude via the normalization. Following a suggestion by King and van Vleck [26], the renormalization is accounted for by the two parameters λ_s and λ_p defined as

$$\lambda_s^2 = |^1\psi(0)|^2 \,/\, |^3\psi(0)|^2 \qquad (8a)$$

$$\lambda_p^2 = {}^1\langle r^{-3}\rangle \,/\, {}^3\langle r^{-3}\rangle \qquad (8b)$$

This modification led to a consistent description of the fs and hfs splittings in sp configurations [6,7,27]. Obviously the different single-electron hfs constants in the pure singlet and triplet states and their off-diagonal matrix elements (indicated by the double index ^{13}) are interrelated as

$$^{13}a_s = \lambda_s \, ^3a_s \tag{9a}$$

$$^1a_{pj} = \lambda_p \, ^{13}a_{pj} = \lambda_p^2 \, ^3a_{pj} \tag{9b}$$

$$^1b_{pj} = \lambda_p \, ^{13}b_{pj} = \lambda_p^2 \, ^3b_{pj} \tag{9c}$$

^1a_s does not appear in the formulae, since the spins are coupled to zero in the pure singlet state.

With these definitions the MBWT equations read [7]:

$$A(^3P_2) = (1/4) \, ^3a_s + (3/4) \, ^3a_{p3/2} \tag{10a}$$

$$\begin{aligned} A(^3P_1) = {} & \alpha^2 \{(1/4) \, ^3a_s + [(5/12)-(5\xi/24)] \, ^3a_{p3/2} + (1/3) \, ^3a_{p1/2}\} \\ & + (2/3)\sqrt{2} \, \alpha\beta\{-(3/4)\lambda_s \, ^3a_s + [(5/4)-(5\xi/32)]\lambda_p \, ^3a_{p3/2} \\ & - (1/2)\lambda_p \, ^3a_{p1/2}\} + \beta^2 \{[(5/6)+(5\xi/24)]\lambda_p^2 \, ^3a_{p3/2} \\ & + (1/6)\lambda_p^2 \, ^3a_{p1/2}\} \end{aligned} \tag{10b}$$

$$B(^3P_2) = \, ^3b_{p3/2} \tag{11a}$$

$$B(^3P_1) = (1/3) \{\alpha^2[(1/2)-2\eta] + \sqrt{2} \, \alpha\beta(1-\eta)\lambda_p + \beta^2(1+2\eta)\lambda_p^2\} \, ^3b_{p3/2} \tag{11b}$$

$A(^1P_1)$ and $B(^1P_1)$ instead of $A(^3P_1)$ and $B(^3P_1)$ are obtained by replacing α by $\alpha' = -\beta$ and β by $\beta' = \alpha$. In principle equations (10b) and (11b) contain also off-diagonal matrix elements $a_{\ell+1/2,\ell-1/2}$, $b_{\ell+1/2,\ell-1/2}$. In the frame of the MBWT they are expressed in terms of the diagonal ones with the relativistic corrections ξ and η. The a_{pj} factors for pure configurations are related by the ratio of the relativistic correction functions $F_j(Z_i)$ according to

$$\gamma = a_{p1/2}/a_{p3/2} = 5(1-\delta_{p1/2}) \, (1-\epsilon_{p1/2}) \, F_{1/2}(Z_i)/F_{3/2}(Z_i) \tag{12}$$

3.2 MBWT Analysis of the 7s7p Configuration in Ra I

3.2.1 Mixing Coefficients and Relativistic Corrections

A semi-empirical determination of the mixing coefficients is possible from the deviation of the fine structure intervals from their LS-coupling limit [7] by

$$\beta/\alpha = \{\Delta_o/[E(^1P_1)-E(^3P_1)-\Delta_o]\}^{1/2} \qquad (13)$$

with $\Delta_o = \{[E(^3P_2)-E(^3P_0)]/3\} - \{E(^3P_1)-E(^3P_0)\}$. Inserting term values from [2] yields $\alpha = 0.979$, $\beta = -0.205$ and $c_1 = 0.398$, $c_2 = 0.918$. These values remain unchanged by the inclusion of spin-other orbit and spin-spin interactions, because the corresponding corrections to (13) cancel out [27]. The values are well reproduced by a recent Multi-Configuration Dirac-Fock (MCDF) calculation [9] in which the 7s7p configuration is constructed from a basis of five jj-coupled states $|7s_{1/2},7p_{1/2}>$, $|7s_{1/2},7p_{3/2}>$, $|7p_{1/2},6d_{3/2}>$, $|7p_{3/2},6d_{3/2}>$ and $|7p_{3/2},6d_{5/2}>$, to include the admixtures of the close lying 7p6d configuration. For the evaluation of c_1 and c_2 these additional contributions are projected back into the basis of the two 7s7p configurations which gives $c_1^{th} = 0.425$ and $c_2^{th} = 0.905$. In the frame of this analysis the semi-empirical results will be used.

The relativistic and finite size corrections appearing in the different equations are taken from the standard formulae and tables given e.g. in [22,24,28]. A complete list of parameters used is given in Table 3.

3.2.2 Determination of λ_p

a) λ_p from the Fine Structure: The quantity λ_p appears in the fs as the ratio between the off-diagonal parameter $^{13}\zeta$ and the diagonal parameter $^3\zeta$ of the spin-orbit interaction [6]. A simple approach starts from the experimental term energies as

$$\lambda_p(fs) = {}^{13}\zeta / {}^{3}\zeta \qquad (14)$$
$$= 3\,\{\Delta_o[E(^1P_1)-E(^3P_1)-\Delta_o]\}^{1/2} / \sqrt{2}[E(^3P_2)-E(^3P_0)]$$

and yields $\lambda_p(fs) = 0.792$. An estimation of spin-other orbit and spin-spin interactions according to formulae (19.59), (33.32) of ref. [29], leads to a correction of + 5.1 % in the fine structure interval $E(^3P_2)-E(^3P_0)$ and a corrected $\lambda_p(fs)_c = 0.753$.

b) λ_p from the B-Factors: λ_p can also be determined from the experimental B-factors. Adding up equations (11) gives

$$\lambda_p(hfs) = \{[3[B(^1P_1)+B(^3P_1)]/B(^3P_2) - (1/2) + 2\eta] / [1+2\eta]\}^{1/2} \qquad (15)$$

and the numerical value $\lambda_p(hfs) = 0.742(2)$. The error includes only the experimental uncertainties of the B-factors. A variation of 5 % in η would be reflected in a change of 1 % in $\lambda_p(hfs)$.

Both evaluations give almost identical λ_p values. The systematic difference between $\lambda_p(fs)$ and $\lambda_p(hfs)$, already found in most other alkaline-earth systems by Kluge and Sauter [7], has been removed by the correction due to spin-other orbit and spin-spin interaction. The consistency demonstrates that configuration interactions are effectively included in the MBWT.

3.2.3 Determination of λ_s

The influence of λ_s on the fs splitting is practically negligible. However, through $|\psi_s(0)|^2$ it affects the large contact contribution to the magnetic hfs as well as the isotope shift.

a) λ_s from the Isotopic Field Shift Ratio: Brix and Steudel [30,31] already ascribed the small difference between the isotopic field shifts of the two resonance lines from the $^1S_0$ to the $^1P_1$ and $^3P_1$ states to a different density $|\psi_s(0)|^2$ of the s-valence electron in the excited states, i.e. to λ_s. However, also the p electron contributes namely by its own charge density $|\psi_p(0)|^2$ and by interaction with closed s-shells

(screening). Semi-empirically we can account for the first two effects (whereas the last one is accessible only to ab-initio calculations). In this approximation the ratio of the field shifts is

$$\rho_{4826,7141} = \frac{F_{4826}}{F_{7141}} = \frac{\Delta|\psi(0)|^2_{4826}}{\Delta|\psi(0)|^2_{7141}} = \tag{16}$$

$$= \frac{|\psi(0)|^2_{7s^2} - (\lambda_s^2|\psi(0)|^2_{7s} + c_1^2|\psi(0)|^2_{7p1/2})}{|\psi(0)|^2_{7s^2} - (|\psi(0)|^2_{7s} + c_2^2|\psi(0)|^2_{7p1/2})}$$

We take the assumption $|\psi(0)|^2_{7s^2} = 1.8(2)\ |\psi(0)|^2_{7s}$ which is based on systematics [31] and confirmed by MCDF calculations [32]. The ratio $|\psi(0)|^2_{7p1/2}/|\psi(0)|^2_{7s} = 0.07(1)$ is calculated according to [19]. Inserting the experimental value ρ_{ij} from Table 7 and the mixing coefficients c_i finally yields $\lambda_s(IS) = 1.03(2)$.

b) λ_s from ab-initio Calculations: The MCDF-calculations of relativistic charge densities in Ra give direct theoretical access to λ_s. In the five-configuration ansatz [9] the contribution of the 7s electron to the total charge density is calculated to be 807 a_o^{-3} in the singlet and 798 a_o^{-3} in the triplet state [32]. This gives $\lambda_s(MCDF) = 1.01$. The error of this result is difficult to estimate.

Due to the large number of parameters in the MBWT description of the magnetic hfs, λ_s can not be determined independently from the experimental A-factors. Therefore we use the value $\lambda_s(IS) = 1.03(2)$.

3.3 Quadrupole Coupling Constants

With the mixing coefficients and relativistic corrections given in Table 3 equations (11a,b) relate three experimental B_j-factors to only two free parameters, λ_p and $^3b_{p3/2}$. This overdetermination offers the chance to prove the validity of the description.

The results of a fit of all 7s7p hfs with the single free parameter $^3b_{p3/2}$ are given in Table 4, in comparison with the experimental numbers. The agreement within the experimental errors is excellent. For the sake of comparison the results of the original Breit-Wills theory ($\lambda_p = 1$) are also included in Table 4. They deviate from MBWT and the experiment by about 30 %.

3.4 Magnetic hfs Constants

The set of equations (11) relates three experimental A_j-factors to three one-electron hfs constants a_s, $a_{p3/2}$, $a_{p1/2}$. Thus the latter ones can be calculated unambiguosly, but there is no overdetermination for a consistency check. With the parameters α, β, λ_p, λ_s, ξ from Table 3, we obtain the $a_{\ell j}$ factors listed in Table 4. Although the magnetic hfs is dominated by the s-electron by orders of magnitude, the small a_p factors still are determined with reasonable precision (2 % for $a_{p1/2}$, 9 % for $a_{p3/2}$). Note that the ratio $\gamma_{ex} = a_{p1/2}/a_{p3/2} = 17.3$ is considerably larger than the theoretical value of 11.8 given in Table 3. The difference is mainly due to the spin-dependent exchange core polarization which is neglected in equations (2) and (12); it will be discussed in the EOF analysis below. Again the original Breit-Wills analysis ($\lambda_s = \lambda_p = 1$) yields distinctly different a-factors, although the change is not as dramatic as for the b-factor.

4. EFFECTIVE OPERATOR FORMALISM (EOF)

4.1 General Presentation

The EOF was introduced 1965 by Sandars and Beck [8]. It gives a correct parametrization of the hfs Hamiltonian in terms of non-relativistic angular momentum operators with a and b factors in which the radial matrix elements are free parameters. Relativistic corrections are included in these parameters. The theory also contains terms representing the effect of exchange core polarization of the inner s shells by the valence electrons. The effective Hamiltonians of magnetic and electric hfs, for each valence electron k, are given as [8,33]:

$$\mathcal{H}^{(1)}_{eff_k} = [T^1_n/(\mu_I/I)] \left\{ \ell_k \, a^{(k)}_{01} - \sqrt{10}\,(s_k C^2_k)^1 \, a^{(k)}_{12} + s_k \, a^{(k)}_{10} \right\} \quad (17a)$$

$$\mathcal{H}^{(2)}_{eff_k} = (T^2_n/eQ_s) \left\{ -C^2_k \, b^{(k)}_{02} + \sqrt{3/10}\, U^{(13)2}_k \, b^{(k)}_{13} + \sqrt{3/10}\, U^{(11)2}_k \, b^{(k)}_{11} \right\} \quad (17b)$$

Here, $T^{(1)}_n$ is the magnetic dipole and $T^{(2)}_n$ the electric quadrupole operator which act on the nucleus. $U^{(ij)2}$ is a double tensor operator of rank i in spin, j in orbital and 2 in combined space, C^2 is the second spherical harmonic. The three terms in the wavy bracket of (17a) represent the orbital, spin-dipolar and contact interaction. The two last terms in the quadrupole interaction are of purely relativistic origin. $U^{(13)2}$ vanishes for $\ell < 2$. All different effective hfs constants a_{ij} and b_{ij} are related to the corresponding radial parameters $\langle r^{-3} \rangle_{ij}$ or hfs fields according to

$$a_{ij} = (2\mu_o\mu_B/4\pi) \langle r^{-3} \rangle_{ij} (\mu_I/I) = \mu_o \langle H^{(0)}_{ij} \rangle \, \mu_I/I \quad (18a)$$

$$b_{ij} = (e^2/4\pi\varepsilon_o) \langle r^{-3} \rangle_{ij} \, Q_s = e \langle \varphi^{(0)}_{zz,ij} \rangle Q_s \quad (18b)$$

The parameters $\langle r^{-3} \rangle_{ij}$ are not related simply to empirical quantities, but accessible only by ab-initio calculations. The effective hfs constants a_{ij} and b_{ij} in a particular configuration are obtained from the experimental A_J and B_J factors by adding the contributions (17) for each valence electron via vector coupling rules [33]. This leads to a set of equations which can be solved only, if a sufficient number of independent A_J, B_J factors are known. Usually the influence of different radial wave functions for different multiplicities is neglected (see e.g. [34]) because the inclusion of this effect strongly increases the number of unknown parameters. This leads to serious inconsistencies. They can be removed by including additional semi-empirical [35] or theoretical [36] information about radial wave functions into the formulae.

4.2 Application of the EOF to the 7s7p Configuration in Radium

a) Hfs-Formulae and Reduction of Parameters: The effective hyperfine hamiltonian for the configuration 7s7p is composed of one term a^s_{10} due to the s electron, (the contact term)

and five terms due to the p electron, namely three a^p_{ij} and two b^p_{ij}. The intermediate character of the coupling is again expressed by intermediate wave functions according to (7). The different radial dependence of the singlet, off-diagonal and triplet terms introduces altogether eight a_{ij} and four b_{ij} parameters facing only three A and three B factors from the experiment. The final EOF expressions for the hfs of a nsnp configuration thus read [36]

$$A(^3P_2) = (1/4)\{^3a^s_{10} + 2\,{}^3a^p_{01} - (2/5)\,{}^3a^p_{12} + {}^3a^p_{10}\} \tag{19a}$$

$$A(^3P_1) = (\alpha^2/4)\{^3a^s_{10} + 2\,{}^3a^p_{01} + 2\,{}^3a^p_{12} + {}^3a^p_{10}\} - (\alpha\beta/\sqrt{2})\{^{13}a^s_{10} + {}^{13}a^p_{12} - {}^{13}a^p_{10}\} + \beta^2\,{}^1a^p_{01} \tag{19b}$$

$$B(^3P_2) = (2/5)\,{}^3b^p_{02} + (1/\sqrt{45})\,{}^3b^p_{11} \tag{20a}$$

$$B(^3P_1) = (-\alpha^2/5)\,{}^3b^p_{02} + (\alpha^2/\sqrt{180})\,{}^3b^p_{11} + (\alpha\beta/\sqrt{90})\,{}^{13}b^p_{11} + (2\beta^2/5)\,{}^1b^p_{02} \tag{20b}$$

$A(^1P_1)$ and $B(^1P_1)$ are obtained by replacing α by $\alpha' = -\beta$ and β by $\beta' = \alpha$ in (19b) and (20b). The superscripts ^{3}, ^{13}, ^{1}, again indicate triplet, off-diagonal and singlet matrix elements. Since no ab-initio calculations are available, the number of parameters is reduced by introducing the semi-empirical quantities $\lambda_p = 0.742(2)$ and $\lambda_s = 1.03(2)$ similar to the MBWT approach. Still the three A factors depend on the four variables $^3a^s_{10}$, $^3a^p_{01}$, $^3a^p_{12}$, $^3a^p_{10}$ and require another input parameter. The safest choice is the ratio γ of the relativistic correction factors F_j (cf. (11)). They depend mostly on the simple, unscreened Coulomb potential close to the nucleus. Furthermore, this ratio is obtained independently from two different ab-initio calculations on the hfs fields, as $\gamma = 11.0(6)$ [11] and $\gamma = 11.7(2)$ [12], in perfect agreement with the semi-empirical $\gamma = 11.8$ [24]. We introduce the theoretical ratio between the orbital and spin-dipole coupling constant which is related to the γ factor by

$$(a^p_{01}/a^p_{12}) = (2 + \gamma/5)/(\gamma - 2) \tag{21}$$

(21) is obtained from (12) and the general relations between the single-electron hfs constants $a_{\ell j}$, $b_{\ell j}$ and the EOF parameters [33]:

$$a_{p1/2} = (1/3)\ \{4\ a^p_{01} + \ \ 4\ \ a^p_{12} - a^p_{10}\} \tag{22a}$$

$$a_{p3/2} = (1/3)\ \{2\ a^p_{01} - (2/5)\ a^p_{12} + a^p_{10}\} \tag{22b}$$

$$a_{p3/2,1/2} = (1/3)\ \{a^p_{01} - (1/2)\ a^p_{12} - a^p_{10}\} \tag{22c}$$

$$b_{p3/2} = (2/5)\ b^p_{02} + (1/\sqrt{45})\ b^p_{11} \tag{22d}$$

$$b_{p3/2,1/2} = (2/5)\ b^p_{02} - (1/\sqrt{180})\ b^p_{11} \tag{22e}$$

where the suffix $_{3/2,1/2}$ denotes the off-diagonal elements. (Note in deriving (21) that the core polarization term a^p_{10} was omitted in the definition of γ by equation (12).)

b) Results and Comparison with the MBWT Analysis:

With this input we calculate the EOF parameters as included in Table 5. They may be transformed back into the usual a_{pj} and b_{pj} factors by use of equations (22). The agreement with those, from the MBWT analysis is perfect. This is not surprising as the MBWT equations (10), (11) and the EOF equations (19), (20) are now fully equivalent. The relativistic corrections ξ and η, entering as fixed quantities into the MBWT, are determined in the EOF as free ratios between the different radial parameters to be ξ = 1.08(4) and η = 1.41(6) in perfect agreement with Table 3.

A closer inspection of equations (19a,b) reveals a direct correlation between the two contact terms $^3a^s_{10}$, $^3a^p_{10}$ and the λ factors: the former occur either as sum $S = {}^3a^s_{10} + {}^3a^p_{10}$ or as difference $D = \lambda_s\ {}^3a^s_{10} - \lambda_p\ {}^3a^p_{10}$. While these two quantities are well determined in the fit, the contribution of the p electron contact term is strongly dependent on λ_s and λ_p, especially as the ratio $^3a^s_{10}/{}^3a^p_{10}$ is of the order 100. In fact, the choice λ_s = 1.06 instead of 1.03 makes $^3a^p_{10}$

vanish whilst the dominating $^3a^s_{10}$ changes by less than 2 % only. Hence we conclude that the evaluation of the exchange core polarization by the p electron remains rather uncertain in a (s,p)-configuration. This is explicitely illustrated in the second errors of the EOF hfs constants, as given in the square brackets in Table 5. These represent the additional uncertainties, apart from the purely experimental errors ascribable to λ_s and λ_p.

The third parameter a^p_{01} is not correlated to the contact terms and, in particular, not influenced by these mutual uncertainties. In conclusion the orbital and (through γ also the) spin-dipolar a-factors are safely evaluated within the frame of both the MBWT and the EOF theories; their accuracy is mainly limited by the experimental errors of the A_J-factors.

5. Hfs-Fields and Nuclear Moments

The magnetic hfs field H(0) and the electric field gradient $\varphi^{(0)}_{22}$ in a term J are traditionally defined by the relations

$$A_J = \mu_I \mu_o \langle H_J(0)\rangle / IJ \qquad (23), \qquad B_J = e\langle \varphi^{(0)}_{zz,J}\rangle Q_s \qquad (24)$$

which are also used to define the single electron hfs fields from the a_j, b_j [22]. In the EOF analysis we use the corresponding definitions (18a,b) instead.

5.1 Magnetic Dipole

a) Ra II Ground State:

The evaluation of $\langle H_J(0)\rangle$ is supposed to be most reliable in the case of a clean, single-valence-electron contact s term such as in the ionic ground state $7s\ ^2S_{1/2}$. Here three independent ab-initio calculations using relativistic many body perturbation theory (RMBPT) are available [10,11,12], while in addition the GFS formula (5a) can be used in a semi-empirical approach. With the latter a charge density value of $|\Psi(0)|^2_{7s} = 10.15\ a_o^{-3}$ is found using the corrections given in Table 3

and the effective quantum number n* = 2.316. This corresponds to a magnetic hyperfine field of B(0) = 1285.(65) Tesla. The error of 5 % is based on empirical evidence from numerous analogue cases, where μ_I is known from independent sources. The number agrees with the different RMBPT calculations which include many-body effects as well as the finite size corrections $(1-\delta)$ $(1-\varepsilon)$ (see Table 5). The remaining difference is much smaller than the many-body effects, namely, the core polarization and correlation terms. These contribute about 33 % to the total hfs field according to the RMBPT calculations [10,11,12]. We conclude that the GFS procedure effectively takes into account these effects, though it certainly does not pretend to do so. The reason for that is not quite clear. The aim of the GFS formula was only to calibrate semi-empirically the density of an one-electron wavefunction within the core. The accidental inclusion of many-body effects indicates that they should scale with that density, or, in other words, that the inner part of the wavefunction is mainly responsible for these many-body contributions. Thus one could account for the many-body effects in an one-electron calculation by the introduction of a simple renormalization factor for the hfs interaction.

b) Ra II 7p $^2P_{1/2}$ State:

The hfs field for the excited 7p $^2P_{1/2}$ state has been calculated semi-empirically from the fs splitting and the p-electron GFS formula. The two resulting magnetic moments show a systematic deviation of about 10 % to higher values (compare Table 5). This fact can be ascribed to the neglection of core polarization contributions, which are similar in the other alkali-like spectra (e.g. in Ba II, Sr II). Due to the lacking $A(^2P_{3/2})$ factor they cannot be accounted for. The admixtures from higher np states, which are due to the strong spin-orbit coupling in high-Z spectra, have also been disregarded because of the limited knowledge about these levels.

The ab-initio results from RMBPT include both effects and thus show complete consistency with the results from the ionic ground state (compare Table 5).

c) Ra I 7s7p Configuration:

The a-factors of the Ra I 7s7p configuration have been tested for their applicability to the determination of nuclear moments via a semi-empirical evaluation of the corresponding hyperfine fields.

In case of the s electron the relation from section 3.2, $|\Psi_s(0)|^2_{7s^2} = 1.8(2)\ {}^3|\Psi_s(0)|^2_{7s7p}$ is used again, taking for $|\Psi_s(0)|^2_{7s^2}$ simply twice the value calculated from equation (4). With $n^* = 1.6054$ and $(1 - d\sigma/dn) = 1.059$ one finally obtains ${}^3|\Psi_s(0)|^2_{7s7p} = 7.97(80)\ a_o^{-3}$. This leads to $\mu_I = 0.267(27)\mu_N$ in perfect agreement with the ionic values (compare Table 5).

For the p electron, the semi-empirical hyperfine field can be evaluated from the corrected fs according to (6) or from the p electron GFS formula (5). The application of the latter to the two-electron system leads to a value of $\langle H_J(0)\rangle$ about 15 % smaller than from the fs. In addition, both numbers fail in the evaluation of μ_I from the MBWT a_p factors, and yield a result, which is about 10 to 25 % smaller than from the ionic a factors (compare Table 5). In a check of the lighter two-electron systems by using the complete MBWT data from [7,37,38,39] a similar discrepancy is found in the case of Ca, Sr and Cd, while only Hg gives consistent results [40]. In Ba no complete MBWT analysis could be performed, due to the missing A-factor of the 6s6p $^3P_2$ state. This more or less general failure in the extraction of μ_I from the MBWT a_p factors seems to be due to an errorneous approach in the determination of the p electron hfs field from thefs in the two-electron system. The consideration of spin-other-orbit and spin-spin interaction contributions to the fs according to [29] slightly increases the discrepancy by 5 %. (The earlier used Wolfe correction [41] is not adequate in the MBWT approach.)

Thus the deviation of μ_I is ascribed to the insufficiency of only one identical parameter $\langle r^{-3}\rangle_p$ for the magnetic hfs of the p electron as well as the two-electron fs.

As already mentioned, this simplification is discarded in the EOF formalism where ab-initio calculations of the radial parameters avoid the introduction of empirical quantities. MCDF calculations of the radial EOF parameters $\langle r^{-3}\rangle_{ij}$ have recently been performed by Büttgenbach [42]. Using a simple basis of only two jj-coupled configurations $|7s_{1/2}, 7p_{1/2}\rangle$, $|7s_{1/2}, 7p_{3/2}\rangle$ gives the preliminary results for the hfs fields which are included in Table 5. The μ_I-values calculated from the orbital a^p_{01} factor is identical with the result from the MBWT a_p factors, while the contact and spin-dipolar terms unfortunately deviate strongly, up to 30 %. These discrepancies show that satisfactory ab-initio descriptions for Ra are not yet available. Reliable results are expected from RMBPT approaches and refined MCDF calculations from complete basis systems which include effects like core polarization and correlations in the two-electron systems.

For the time being we choose for the magnetic moment a reference value of $\mu_I(^{223}\mathrm{Ra})=0.2600(5)\mu_N$ which is the weighted average of the four values calculated from the ionic ground state. Its accuracy is expected to be of the order of 2 %. The moments of the other isotopes given in Table 6 are then calculated by the ratio

$$^x\mu_I = {}^{223}\mu_I \{(3/2)\ {}^xA / ({}^{223}A\ {}^xI)\} \qquad (25)$$

where ^xA is the A factor of isotope x and ^xI its spin. Here a possible hfs anomaly is neglected as it is known to be smaller than 0.5 % (compare [1]).

5.2 Electric Quadrupole

As no quadrupole splitting has been measured in the single-electron Ra II spectrum, we have to rely entirely on the MBWT or EOF analysis of the 7s7p configuration of Ra I in extracting Q_s. Both approaches have turned out to be reliable enough to

give safe single electron b-factors $^3b_{p3/2}$ or $^3b_{02}$, respectively, from the three B factors measured. The semi-empirical evaluation of the quadrupole hfs field $\langle\varphi_{zz}(0)\rangle$ according to (24) implies the same p electron radial parameter $^3\langle r^{-3}\rangle_p$ as used for the magnetic interaction. Due to the disagreement of up to 25 % between $\langle r^{-3}\rangle_p$ from GFS formula, fs and magnetic hfs we have three different choices. In the analysis of the lighter two-electron systems Ca I, Sr I, Ba I, Cd I and Hg I usually the value from the fs according to (6) has been used for the electric hfs. Hühnermann has shown explicitely that this choice of $\langle r^{-3}\rangle_p$ yields Q_s values in good agreement with the ones obtained from the clean single electron B factors from the ionic one-electron system [43]. In this way the assumption of identical $\langle r^{-3}\rangle_p$ for fs and electric hfs and a slightly smaller value for the magnetic hfs seems to be justified. We thus rely on this approach, which yields $Q_s = 1.47$ for ^{223}Ra.

In the ab-initio MCDF calculations a preliminary value $^3\langle r^{-3}\rangle_{02} = 4.84\ a_0^{-3}$ has been evaluated for the radial integral of the quadrupolar term [42]. Inserting this into (19b) and using the effective $^3b_{02}$ factor from Table 5 gives $Q_s = 1.9$ b. There is a discrepancy of about 30 % with the semi-empirical value of Q_s, which is again ascribed to the simplifications involved in the constrained two-configuration MCDF ansatz. It is similar in size and direction as the deviation of the contact and spin-dipolar term in the magnetic hfs.

The polarization of the electronic core by the quadrupole field of the nucleus [44] is accounted for by the Sternheimer correction:

$$Q_s^{cor} = Q_s^{uncor}/(1 - R_{7p}) \qquad (26)$$

For the radium 7p levels Sternheimer has estimated a correction factor $R_{7p} = -0.24(5)$ from systematics [45]. The corrected Q_s values obtained from the semi-empirical approach are listed in Table 6 for all isotopes under study. The confidence level ascribed to these numbers is about ≈ 10 %, due to the uncertainties in the radial parameter (5 % - 10 %) and the Sternheimer

correction (5 %). A more reliable and precise value for Q_s is expected from future measurements of the ionic $B(^2p_{3/2})$ factor. Here the radial parameter $\langle r^{-3}\rangle_p$ can be obtained consistently within 3 % by the semi-empirical as well as the ab-initio method.

The results for Q_s as derived independently from the analysis of the Ra I hfs agree very well with the preliminary ones [1]. These were calibrated with reference to Q_s = 2.9 b for the strongly deformed nucleus ^{229}Ra. In the strong-coupling limit this spectroscopic quadrupole moment corresponds to an intrinsic quadrupole moment of Q_o = 8.0 b which is extrapolated from a series of Q_o values from the neighbouring even isotopes ^{222}Ra - ^{228}Ra. They are known from measurements of B(E2) transition strengths with an accuracy of 5 %. The agreement of both results gives confidence into the present semi-empirical evaluation of Q_s as well as the validity of the strong-coupling projection formula for the heaviest Ra isotopes with deformations of about $\beta_2 \approx 0.2$.[1)]

6. Isotope Shifts in Ra II and Ra I

The IS of up to 19 isotopes has been measured in the four transitions. For isotopes with mass A and A' it is conventionally expressed as a sum of the field shift (FS) and the mass shift which again is decomposed into the normal mass shift (NMS), represented by the constant $N_i = \nu_i/1836.1$, and the specific mass shift (SMS), represented by S_i:

$$\delta\nu_i^{AA'} = F_i\,\lambda^{AA'} + \{N_i + S_i\}\,(A'-A)/AA' \quad . \tag{27}$$

1) The extrapolation of Q_o from ^{228}Ra to ^{229}Ra is still a bit ambigous, in particular since some discontinuity towards larger deformation values is expected around N = 142 (corresponding to ^{230}Ra) [13]. By comparison with the isotonic ^{232}Th (Q_o = 9.7 b [46]), one is also tempted to assume a Q_o value of ^{229}Ra slightly larger than 8 b.

The field shift is the product of an electronic factor F_i and the nuclear parameter $\lambda^{AA'}$ which differs from the (usually discussed) change in the mean-squared nuclear charge radius $\delta\langle r^2\rangle^{AA'}$ by a correction for higher radial moments [47]

$$\lambda^{AA'} = \delta\langle r^2\rangle^{AA'} + \sum_n \frac{C_n}{C_1} \delta\langle r^{2n}\rangle^{AA'} . \qquad (28)$$

The following discussion is confined to an analysis of (27), whereas the nuclear physics interpretation will be given elsewhere.

6.1 Ra II Resonance Line

The well-known semi-empirical approach [48] is applied to the alkali-like s-p transition of Ra II. F(4683 Å) is written as

$$F(4683\ \text{Å}) = a_0^3/Z \{\Delta|\Psi(0)|^2\}_{4683} f(Z,A) \qquad (29)$$

with the (non-relativistic) change of the electronic charge density in the transition and the parameter f(Z,A). The latter contains relativistic corrections and the influence of the finite size of the nucleus on the electronic wavefunction. A recent recalculation of this quantity has been given by Blundell et al. [49]. The change of the electronic charge density $\Delta|\Psi(0)|^2$ during the optical transition is given as a fractional part of the dominant charge density in the s-state

$$\{\Delta|\Psi(0)|^2\}_{s-p} = ß\ |\Psi(0)|^2_s \qquad (30)$$

Ab-initio calculations of the screening factor ß have proved to be reliable. Recent Dirac-Fock (DF) calculations in Ra II give ß = 1.039 for the $7s-7p_{1/2}$ transition [9]. With the use of the semi-empirical charge density $|\Psi(0)|^2_{7s} = 10.15\ a_0^{-3}$ (cf. Section 5.1), F(4683 Å) is determined to be

$$F(4683\ \text{Å})_{se} = -49.2\ \text{GHz/fm}^2$$

for the isotope pair ^{224}Ra - ^{226}Ra (with $f(88,225) = c_{unif}/\lambda_{unif}$ = - 120.95 GHz/fm²). The DF calculations of Torbohm et al. [9] give an ab-initio value of

$$F(4683\ \text{Å})_{DF} = -\ 39.5\ \text{GHz/fm}^2.$$

For both values the mass dependence as given in [49] has to be considered for the further evaluation. Due to the lack of an independently determined magnetic moment in radium, the third possibility for a determination of F(4683 Å) from the hfs formula (4a) has not been used. The two different F values show a disagreement of about 20 %. In the other alkaline earth elements the discrepancy between ab-initio and semi-empirical values of F is of the same order (e.g. for Ba: 25 % and Sr: 21 %), always showing the same direction with smaller ab-initio values. The reasons for this disagreement are not yet understood (compare the discussion in [9,15]). Thus the ultimate choice of F, necessary for the determination of absolute $\delta\langle r^2\rangle$ values, will be left over to the forthcoming publication on the nuclear physics of radium.

6.2 Ratios of Electronic Field Shifts

In a comparison between different optical transitions i and j the field and mass shifts can be separated by a King-plot. Based on the linear dependence of the field shift $\delta\nu_{FS_i}$ on the nuclear parameter $\lambda^{AA'}$ one derives

$$\delta\nu^{AA'}_{j,King} = (F_j/F_i)\delta\nu^{AA'}_{i,King} + S_j - (F_j/F_i)S_i \qquad (31)$$

between the transformed IS

$$\delta\nu^{AA'}_{King} \equiv \delta\nu^{AA'}\{AA'/(A'-A)\} - N. \qquad (32)$$

Plotting (31) for all pairs measured and fitting a straight line to the data yields the ratio of the FS as the slope

$$\varrho_{ij} = F_j/F_i \qquad (33a)$$

and the difference of the SMS as the abscissa

$$D_{ij} = S_j - \varrho_{ij} S_i \,. \tag{33b}$$

The King plot for the 4826 Å line in Ra I against the 4683 Å line in Ra II is given in Fig. 4. It perfectly reproduces a straight line for all 16 data pairs within their extremely small errors of about 3×10^{-4}. The experimental error bars are shown in the inlays with an enlargement of a factor 100. The two other plots between the 4826 Å line and the 7141 Å and 6446 Å show the same precision. The results for ϱ_{ij} and D_{ij} are listed in Table 7.

This table also includes theoretical values for ϱ_{ij} from the DF and MCDF calculations [9]. The theory perfectly reproduces the experimental ratio $\varrho(4826,4683)$. For the ratio $\varrho(4826,7141)$ there is only a slight discrepancy of about 3 %. The experimental ratio $\varrho(4826,7141) > 1$ indicates slightly larger charge density in the singlet state $7s7p\ ^1P_1$ than in the triplet state $7s7p\ ^3P_1$ (compare the discussion on λ_s), while the theoretical prediction postulates the contrary. This discrepancy shows that so far the LS dependent many-body effects are not perfectly reproduced by the MCDF ansatz. A theoretical value for $\varrho(4826,6446)$ is not available.

6.3 Differences of Specific Mass Shifts

The differences of the SMS factors D_{ij}, as given in Table 7, are all consistent with zero within their errors. These errors amount to between 10 % and 40 % of the normal mass shifts. Therefore no direct conclusion about relative direction or magnitude of the specific mass shift parameters S_i can be drawn. Theoretical calculations of mass shifts in radium are missing completely. However, the small specific mass shift differences between ionic 4683 Å and atomic 4826 Å lines and also between the atomic 4826 Å and 7141 Å lines are well within the range usually observed for s, p, s^2 and sp configurations [48]. One assumes, therefore, that also their total specific mass shift is smaller than the normal one.

With this assumption we conclude that also the 7s7d $^3D_3$ state has only a small specific mass effect. On the other hand, transitions involving states of a np(n-1)d configuration show huge specific mass effects ($S_i \gtrsim 100\ N_i$) which indicate strong correlations between the electron momenta. This is a characteristic phenomenon of inner d and f shells, but seems to vanish already in the next higher-n shell. For the evaluation of $\lambda^{AA'}$ in Ra uncertainties of the specific mass shifts are of minor importance. A change in the SMS value S_i of about N_i would result in a variation of less than 1 % in all $\lambda^{AA'}$ values.

7. Conclusion and Outlook

The hfs and IS in one Ra II and three Ra I transitions, involving all low lying sp states, have been studied. The hfs of this configuration is well-described by the semi-empirical Breit-Wills theory in its modified version as well as by the effective operator formalism. Even though large relativistic corrections are involved due to the high Z value of radium, there are no indications for a limit of the semi-empirical approach. The application of the effective operator approach to the 7s7p configuration of radium so far involves different simplifications in the ansatz as well as in the ab-initio calculations of effective radial parameters. While semi-empirical as well as ab-initio calculations of hyperfine fields for the single electron spectrum of Ra II are completely consistent, discrepancies of about 20 % are found in the case of the p-electron hyperfine field of the two-electron system Ra I. This quantity cannot be determined with satisfactory precision by semi-empirical methods. Refined ab-initio approaches might solve this problem.

The independent determination of Q_s and μ_I will be possible via two additional measurements, which are being prepared:

a) The nuclear g_I factor and thus the magnetic moment μ_I will be measured directly by Larmor precession in an external magnetic field by comparison with the precession frequency of a species with known g_I factor [50].

b) The optical study of the ionic 7s $^2S_{1/2}$ - 7p $^2P_{3/2}$ transition at 3918 Å will give the pure $b_{p3/2}$ factor of Ra II and thus allow a direct determination of Q_s from the one electron spectrum as well as further comparisons with the hyperfine parameters discussed in the present paper. This transition in the near UV will be accessible in the near future by the use of the frequency-doubled light of a cw ring dye laser.

The complementary information obtained on the IS of the transitions under study confirms the results from recent MCDF calculations, especially their relative size and extends the experimental basis for an improved theory for the field shift in general.

Acknowledgement

The authors are indebted to T.P. Das, H.T. Duong, C. Ekström, H.-J. Kluge and G. Ulm for their constant encouragement and many fruitful discussions. We gratefully acknowledge the valueable contributions from S. Büttgenbach, who carried out MCDF calculations on radial parameters. B. Fricke kindly provided unpublished material on charge densities in Ra I.

This work has been supported by the Deutsche Forschungsgemeinschaft and the Bundesministerium für Forschung und Technologie. One of us (H.H.S.) acknowledges support from the National Science Foundation under Grant PHY 8503971.

References

[1] Ahmad, S.A., Klempt, W., Neugart, R., Otten, E.W., Wendt, K., Ekström, C., Phys. Lett. 133B, 47 (1983)

[2] Rasmussen, E., Z. Physik 86, 24 (1933); 87, 607 (1934)

[3] Russell, H.N., Phys. Rev. 46, 989 (1934)

[4] Leander, G.A., Sheline, R.K., Nucl. Phys. A413, 375 (1984)

[5] Ragnarsson, I., Phys. Lett. 130B, 353 (1983)

[6] Lurio, A., Phys. Rev. 142, 46 (1966)

[7] Kluge, H.J., Sauter, H., Z. Physik 270, 295 (1974)

[8] Sandars, P.G.H., Beck, J., Proc. Roy. Soc. A 289, 97 (1965)

[9] Torbohm, G., Fricke, B., Rosén, A., Phys. Rev. A31, 2038 (1985)

[10] Das, T.P., private communication and to be published

[11] Heully, J.L., Martensson-Pendrill, A.M., Phys. Scri., 31, 169 (1985)

[12] Dzuba, V.A., Flambaum, V.V., Sushkov, O.P., Phys. Scr. 32, 507 (1985)

[13] Ahmad, S.A., Klempt, W., Neugart, R., Otten, E.W., Wendt, K., Ekström, C., to be published

[14] Ahmad, S.A., Klempt, W., Neugart, R., Otten, E.W., Wendt, K., Proceedings of the 7th International Conference on Atomic Masses and Fundamental Constants (AMCO-7), Darmstadt-Seeheim 1984

[15] Mueller, A.C., Buchinger, F., Klempt, W., Otten, E.W., Neugart, R., Ekström, C., Heinemeier, J., Nucl. Phys. A 403, 234 (1983)

[16] Ravn, H.L., Phys. Reports 54, 201 (1979)

[17] Anton, K.R., Kaufman, S.L., Klempt, W., Moruzzi, G., Neugart, R., Otten, E.W., Schinzler, B., Phys. Rev. Lett. 40, 642 (1978)

[18] Buchinger, F., Mueller, A.C., Schinzler, B., Wendt, K., Ekström, C., Klempt, W., Neugart, R., Nucl. Instr. and Meth. 202, 159 (1982)

[19] Wendt, K., Ahmad, S.A., Buchinger, F., Mueller, A.C., Neugart, R., Otten, E.W., Z. Physik A 318, 125 (1984)

[20] Lurio, A., Mandel, M., Novick, R., Phys. Rev. 126, 1758 (1962)

[21] Breit, G., Lawrence, A.W., Phys. Rev. 44, 470 (1933)

[22] Kopfermann, H., Nuclear moments (Academic Press, New York, 1958)

[23] Casimir, H.B.G., On the Interaction between Atomic Nuclei and Electrons, Teylers Tweede Genotschap, Haarlem, 1932; new Ed. W.H. Freeman Comp, San Fransisco 1963

[24] Schwartz, C., Phys. Rev. 97, 380 (1955) and 105, 173 (1957)

[25] Hartree, D.R., Hartree, W., Proc. Roy. Soc. A 164, 167 (1938)

[26] King, G.W., Van Vleck, J.H., Phys. Rev. 56, 464 (1939)

[27] Vainshtein, L.A., Poluektov, I.A., Opt. Spectr. USSR 12, 254 (1962)

[28] Rosenberg, H.J., Stroke, H.H., Phys. Rev. A5, 1992 (1972)

[29] Sobel'man, I.I.: Introduction to the Theory of Atomic Spectra, Pergamon Press, Oxford (1972)

[30] Brix, P., Z. Physik 132, 579 (1952)

[31] Steudel, A., in: Krebs, K., Nelkowski, H., Z. Physik 145, 543 (1956)

[32] Fricke, B., private communication

[33] Lindgren, I., Rosén, A., Case Studies in Atomic Physics 4, 93 (1974)

[34] Büttgenbach, S.: Hyperfine structure in 4d and 5d shell atoms, Springer-Verlag, Berlin, 1982

[35] Bauche, J., Couarraze, G. Labarthe, J.J., Z. Physik 270, 311 (1974)

[36] Olsson, G., Salomonson, S., Z. Physik A 307, 99 (1982)

[37] Arnold, M., Kowalski, J., Stehlin, T., Träger, F., zu Putlitz, G., Z. Physik A 314, 303 (1983)

[38] Grundevik, P., Gustavsson, M., Lindgren, I., Olsson, G., Robertsson, L., Rosén, A., Swanberg, S., Phys. Rev. Lett. 42, 1528 (1979)

[39] Heider, S.M., Brink, G.O., Phys. Rev. A 16, 1371 (1977)

[40] Ulm, G., Bhattacherjee, S.K., Dabkiewicz, P., Huber, G., Kluge, H.-J., Kühl, T., Lochmann, H., Otten, E.W., Wendt, K., Ahmad, S.A., Klempt, W., Neugart, R. submitted to Z. Phys. A

[41] Wolfe, H.C., Phys. Rev. 41, 443 (1932)

[42] Büttgenbach, S.,private communication

[43] Becker, W., Fischer, W., Hühnermann, H., Z. Physik 216, 142 (1968)

[44] Sternheimer, R.M., Phys. Rev. 80, 102 (1950) and Phys. Rev. 146, 140 (1966)

[45] Sternheimer, R.M., private communication

[46] Loebner, K.E.G., Vetter, M., Hönig, V., Nucl. Data Tables A 7, 495 (1970)

[47] Seltzer, E.C., Phys. Rev. 188, 1916 (1969)

[48] Heilig, K., Steudel, A., At. Data Nucl. Data Tables 14, 613 (1974)

[49] Blundell, S.A., Baird, P.E.G., Palmer, C.W.P., Stacey, D.N., Woodgate, G.K., Zimmermann, D., Z. Physik A 321, 31 (1985)

[50] Bendali, N., Duong, H.T., Saint-Jalm, J.M., Vialle, J.L., J. Physique, 45, 421 (1984)

Table 1: Isotope shifts in the lines under study, relative to the isotope ^{214}Ra. All values in MHz.

	$\delta\nu^{214,A}$ (MHz)			
A	4826 Å	4683 Å	7141 Å	6446 Å
208	8485.(8.)	11950.(8.)	-	-
209	8313.(8.)	-	-	-
210	6003.(6.)	8449.(6.)	-	-
211	5522.(4.)	7770.(4.)	-	-
212	3256.(3.)	4583.(3.)	3303.(5.)	-887.(4.)
213	2167.(3.)	3049.(3.)	-	-
214	0.	0.	0.	0.
220	-21904.(8.)	-30808.(14.)	-	-
221	-25945.(8.)	-36496.(14.)	-	7001.(7.)
222	-28827.(8.)	-40552.(14.)	-29253.(9.)	7781.(4.)
223	-32453.(9.)	-45657.(16.)	-32934.(10.)	8762.(6.)
224	-35123.(9.)	-49411.(16.)	-35644.(11.)	9481.(5.)
225	-38888.(10.)	-54710.(18.)	-39465.(12.)	-
226	-41124.(11.)	-57852.(18.)	-41733.(12.)	11102.(6.)
227	-43937.(12.)	-61811.(19.)	-	-
228	-46950.(12.)	-66050.(20.)	-	-
229	-50066.(15.)	-70432.(22.)	-	-
230	-53634.(15.)	-75456.(23.)	-	-
232	-59585.(17.)	-	-	-

Table 2: Spins and experimental A and B factors for the odd isotopes in all the levels under study. All values given in MHz.

A	209	211	213	221	223	225	227	229
I	5/2	5/2	1/2	5/2	3/2	1/2	3/2	5/2
$A(^2S_{1/2})$	-	6624.8	22920.	-1345.0	3398.3	-27684.	-5063.5	3789.7
		(1.0)	(6.)	(1.8)	(2.9)	(13.)	(3.1)	(2.3)
$A(^2P_{1/2})$	-	1299.7	4525.	-266.3	667.1	-5446.	-996.2	743.9
		(0.8)	(5.)	(1.5)	(2.1)	(7.)	(2.3)	(1.2)
$A(^1P_1)$	-656.5	-668.4	-2314.8	136.3	-344.5	2796.5	512.5	-382.7
	(1.2)	(0.9)	(2.5)	(0.8)	(0.9)	(2.5)	(2.3)	(1.4)
$A(^3P_1)$	-	-	-	-475.8	1202.1	-9793.9	-	-
				(1.4)	(0.6)	(4.3)		
$A(^3P_2)$	-	-	-	278.6	699.6	-	-	-
				(0.9)	(3.3)			
$A(^3D_3)$	-	-	-	213.3	535.6	-	-	-
				(0.6)	(4.6)			
$B(^1P_1)$	135.	162.	-	669.6	421.5	-	531.	1042.
	(5.)	(4.)		(3.0)	(1.6)		(5.)	(5.)
$B(^3P_1)$	-	-	-	-747.6	-470.2	-	-	-
				(2.6)	(1.2)			
$B(^3P_2)$	-	-	-	1103.8	688.5	-	-	-
				(3.9)	(4.0)			
$B(^3D_3)$	-	-	-	117.8	73.9	-	-	-
				(4.4)	(3.0)			

Table 3: Spectroscopic parameters as calculated, and relativistic and finite size corrections for the 7s7p configuration in the modified Breit-Wills scheme, taken from [22,24,28].

α	= 0.979	β	= -0.205
λ_s	= 1.03(2)	λ_p	= 0.742(2)
$F_{s1/2}$	= 3.10	$F_{p1/2}$	= 2.75
$\{1-\delta\sigma/\delta n\}_{s1/2}$	= 1.12	$Fp_{3/2}$	= 1.09
$Z_i(s_{1/2})$	= 88.	$Z_i(p_{1/2})$	= 84.
$\{1-\delta\}_{s1/2}$	= 0.82	$\{1-\delta\}_{p1/2}$	= 0.95
$\{1-\varepsilon\}_{s1/2}$	= 0.96	$\{1-\varepsilon\}_{p1/2}$	= 0.99
ξ	= 1.09	η	= 1.40
H_r	= 1.34	R_r	= 1.29
γ	= 11.8	$\delta\nu_{so}$	= 3800.cm^{-1}

Table 4: Comparison of experimental and calculated A_J and B_J factors from the modified and the original Breit-Wills theory. The values are given for ^{223}Ra (in MHz).

Factor	Experiment	F i t of the B factors	
		mod. B-W λ_p=0.742(2)	orig. B-W λ_p=1.
$B(^3P_2)=^3b_{p3/2}$	688.5(4.0)	693.6(1.5)	514. (32.)
$B(^3P_1)$	-470.2(1.2)	-469.7(1.0)	-331. (21.)
$B(^1P_1)$	421.5(1.6)	421.4(2.5)	588. (37.)
		Calculation of the A factors	
		mod. B-W λ_s=1.03(2) λ_p=0.742(2)	orig. B-W λ_s=1. λ_p=1.
a_s	2668.[1]	2736.(8.)	2908.(44.)
$a_{p3/2}$	-	20.8(1.8)	18.5(4.2)
$a_{p1/2}$	-[2]	371.(8.)	218.5(49.2)

1) evaluated from $A(^2S_{1/2})$ of Ra II via the ratio of electronic charge densities.

2) not determined from Ra II, due to uncertainties in core polarization and $\langle r^{-3}\rangle_p$ factors.

Table 5: Compilation of hyperfine constants and fields in Ra II and Ra I and the nuclear moments derived for ^{223}Ra.

Term and hfs factor	Exp. value [MHz]	$\langle H_J(0)\rangle$ [Tesla]	Method, Ref.	μ_I/μ_N
Ra II 7s	3398.3(2.9)	1285.(65)	GFS this work	.260(13)
		1293.(40)	RMBPT [10]	.259(8)
$A(^2S_{1/2})$		1304.(65)	RMBPT [11]	.26(1)
		1266.(13)	RMBPT [12]	.264(3)
Ra II 7p	667.1(2.1)	229.(23)	GFS this work	.287(29)
		214.(22)	fs this work	.299(29)
$A(^2P_{1/2})$		246.(12)	RMBPT [11]	.270(14)
		243.(3)	RMBPT [12]	.267(3)
Ra I 7s7p				
^3a_s	2736.(8)	1009.(50)	GFS this work	.267(14)
$^3a_{p1/2}+{}^3a_{p3/2}$	392.(8)	129.(13)	GFS this work	.240(24)
		141.(15)	fs this work	.213(21)
$^3a^s_{10}$	2747.(4) [50]	1585.	MCDF [42]	.341
$^3a^p_{01}$	79.(1) [5]	66.	MCDF [42]	.237
$^3a^p_{12}$	178.(3) [12]	115.	MCDF [42]	.304
$^3a^p_{10}$	-41.(12) [40]	-14.	MCDF [42]	-

	B factor [MHz]	$\langle r^{-3}\rangle$ [a_o^{-3}]		Q_s [b]
Ra I 7s7p				
$^3b_{3/2}$	688.5(4.0)	3.85(20)	fs this work	1.20(6)
$^3b^p_{02}$	2193.(5)	4.84	MCDF [42]	1.56
$^3b^p_{11}$	-1265.(18)	-		-

GFS ≙ Goudsmith-Fermi-Segré formula, fs ≙ fine structure formula

Table 6: Nuclear spins and moments μ_I and Q_s as derived from the hfs in Ra I and Ra II. For the Q_s values the Sternheimer correction is applied.

A	209	211	213	221	223	225	227	229
I	5/2	5/2	1/2	5/2	3/2	1/2	3/2	5/2
μ_I/μ_N	.832(16)	.850(16)	.592(11)	-.174(3)	.262(5)	-.713(13)	-.391(8)	.487(9)
Q_s[b]	.38(4)	.46(5)	-	1.90(20)	1.19(12)	-	1.50(15)	2.96(30)

Table 7: Ratios $\rho_{i\,j}$ of electronic field shift factors F_i and differences in specific mass shift factors D_{ij}. Theoretical ρ_{ij}^{DF} values from [9] are included. For the sake of comparison also the normal mass shift factors N_j are given.

Transitions i	Transitions j	ρ_{ij}	ρ_{ij}^{DF}	D_{ij} (GHz)	N_j (GHz)
Ra I, $^1S_0$-$^1P_1$ (4826 Å)	Ra II, $^2S_{1/2}$-$^2P_{1/2}$ (4683 Å)	1.4062(2)	1.403	-28.(30)	349.
Ra I, $^1S_0$-$^1P_1$ (4826 Å)	Ra I, $^1S_0$-$^3P_1$ (7141 Å)	1.0151(8)	0.986	-155.(130)	229.
Ra I, $^1S_0$-$^1P_1$ (4826 Å)	Ra I, $^3P_2$-$^3D_3$ (6446 Å)	-0.2681(5)	-	28.(88)	253.

Figure Captions:

Fig. 1: a) Part of the energy level scheme of Ra II.
b) Part of the energy level scheme of Ra I.
The transitions under study are indicated. Note the enlarged inlay to show the closeness of the 7s7d $^3D_3$ and the neighbouring $^1D_2$ state, giving rise to strong second order hfs perturbation. On the right hand side the ionization energy of Cs (-3.89 eV) and Na (-5.14 eV) is indicated.

Fig. 2: Experimental resonance pattern for the isotope ^{221}Ra (I = 5/2) in the 7s7p $^3P_2$ - 7s7d $^3D_3$ transition (6446 Å). The total angular momentum of upper state and lower state, F_e and F_g are given at the individual hfs components. In addition the center of gravity is indicated by the arrow.

Fig. 3: Positions of the observed resonances relative to ^{214}Ra in the 4683 Å line. Position and length of the horizontal lines represent position and strength of the hfs components for the odd isotopes, while the dots indicate the centers of gravity.

Fig. 4: King plot of the 4827 Å line (horizontal) against the 4683 Å line (vertical). The inlays show the error bares enlarged by a factor of 100.

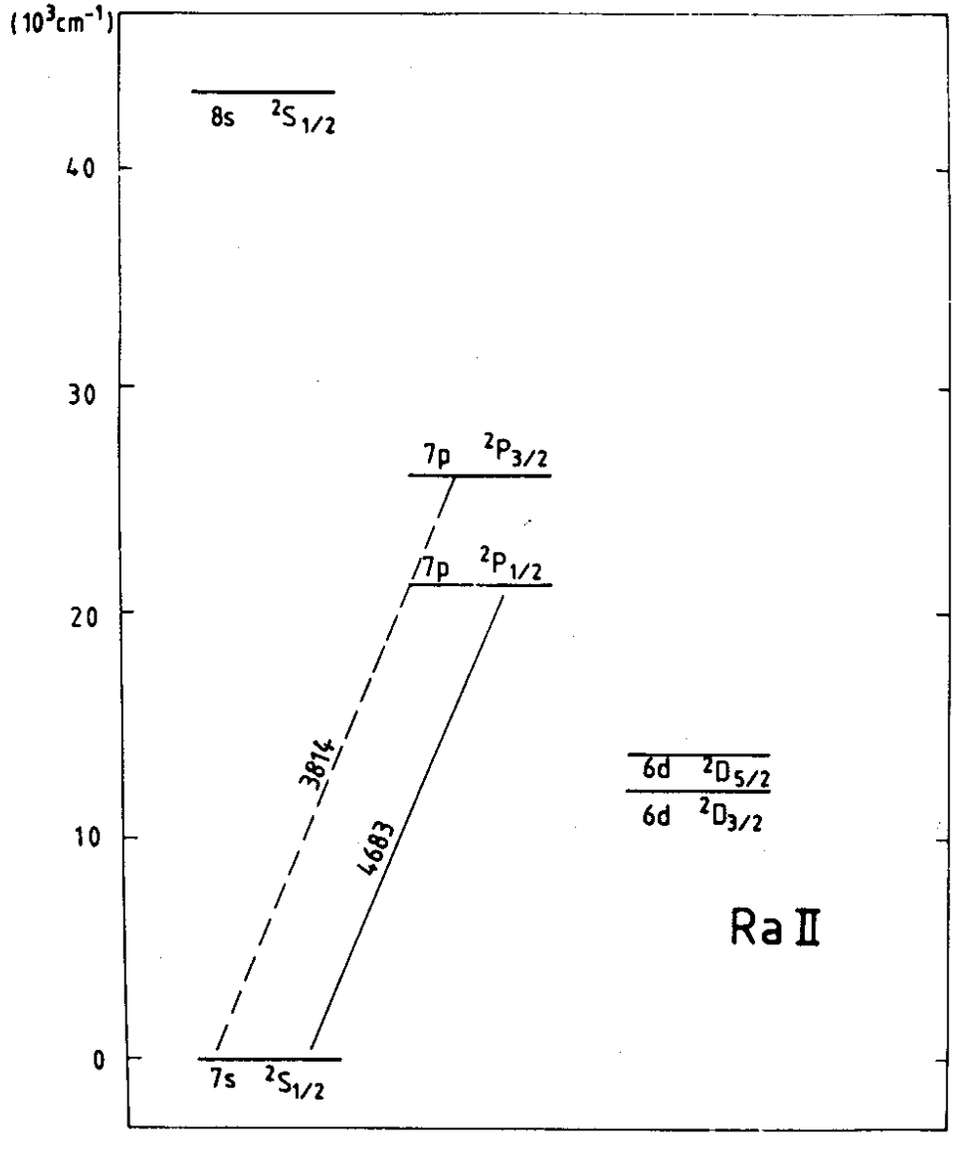
(10³cm⁻¹)
8s ²S1/2
40
30
7p ²P3/2
7p ²P1/2
20
3814
4683
10
6d ²D5/2
6d ²D3/2
0
7s ²S1/2
Ra II

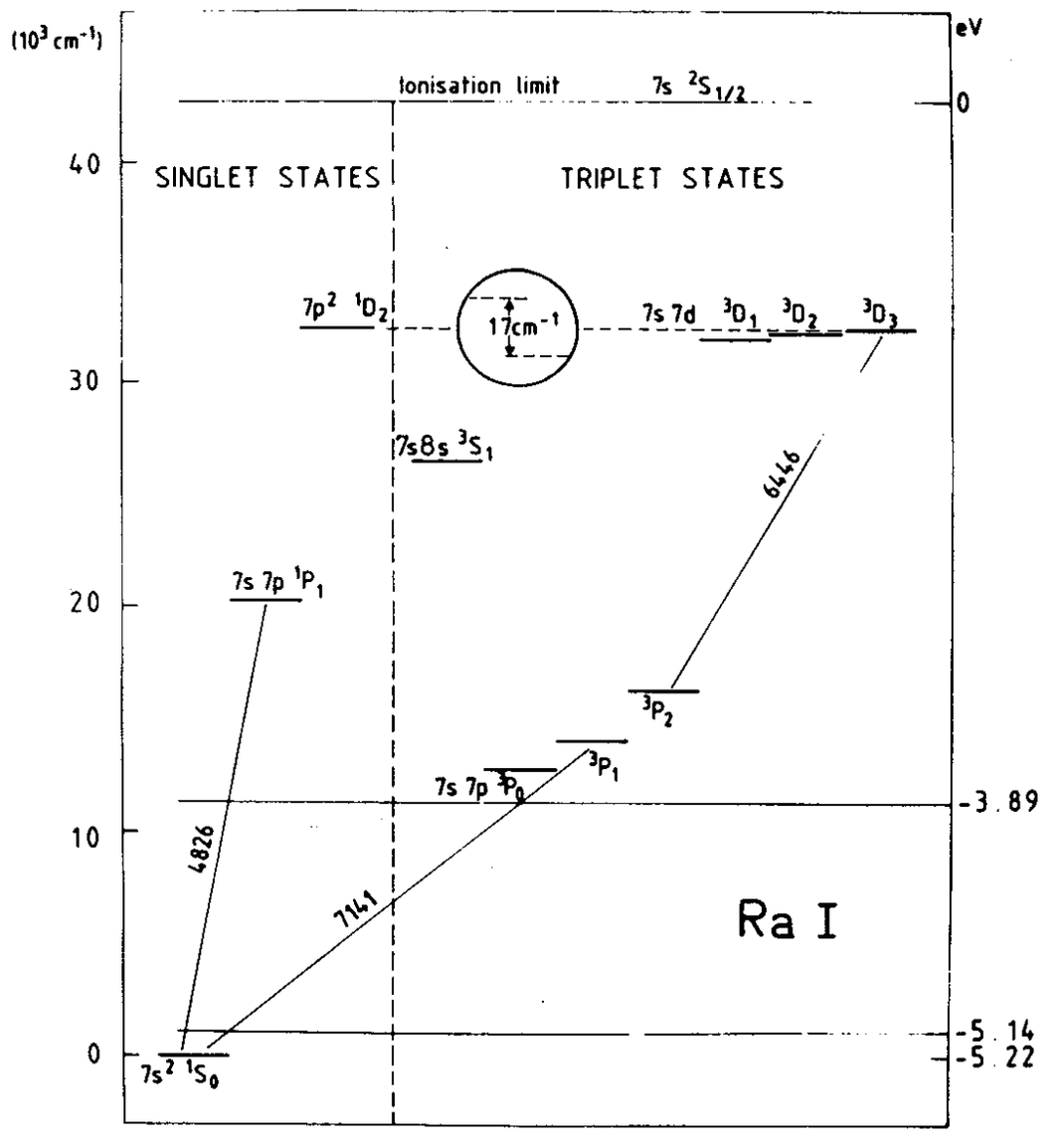
(10³ cm⁻¹)
eV
Ionisation limit
7s ²S1/2
0
40
SINGLET STATES
TRIPLET STATES
7p² ¹D2
17cm⁻¹
7s 7d ³D1 ³D2 ³D3
30
7s8s ³S1
6446
7s 7p ¹P1
20
³P2
³P1
7s 7p ³P0
-3.89
4826
7141
10
Ra I
-5.14
-5.22
0
7s² ¹S0

Fig. 1

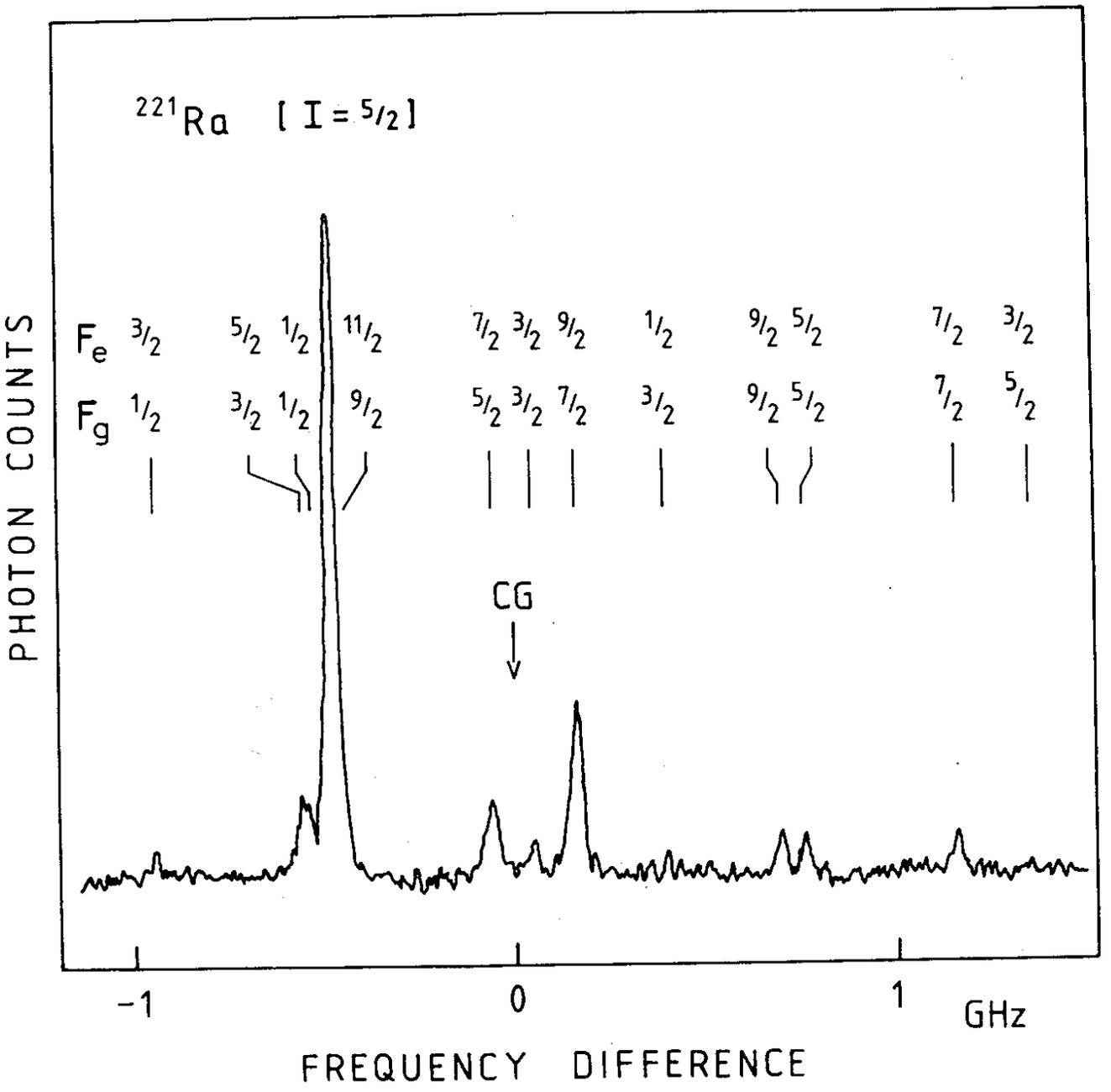
^{221}Ra [I = 5/2]
PHOTON COUNTS
F_e 3/2 5/2 1/2 11/2 7/2 3/2 9/2 1/2 9/2 5/2 7/2 3/2
F_g 1/2 3/2 1/2 9/2 5/2 3/2 7/2 3/2 9/2 5/2 7/2 5/2
CG
-1
0
1
GHz
FREQUENCY DIFFERENCE

Fig. 2

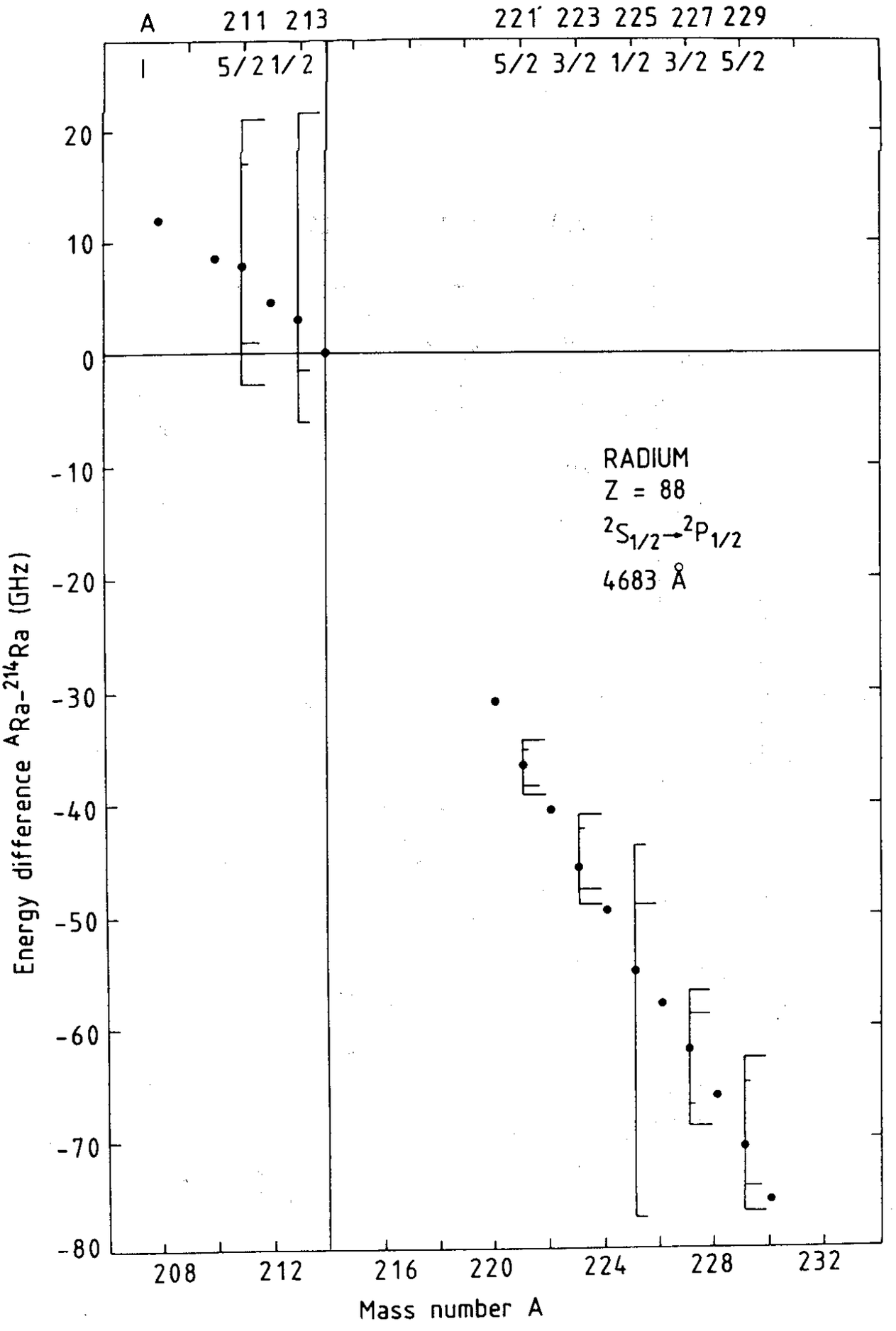
A 211 213 221 223 225 227 229
I 5/2 1/2 5/2 3/2 1/2 3/2 5/2
RADIUM
Z = 88
$^2S_{1/2} \rightarrow {}^2P_{1/2}$
4683 Å
Energy difference ^{A}Ra-^{214}Ra (GHz)
Mass number A
20
10
0
-10
-20
-30
-40
-50
-60
-70
-80
208
212
216
220
224
228
232

Fig. 3

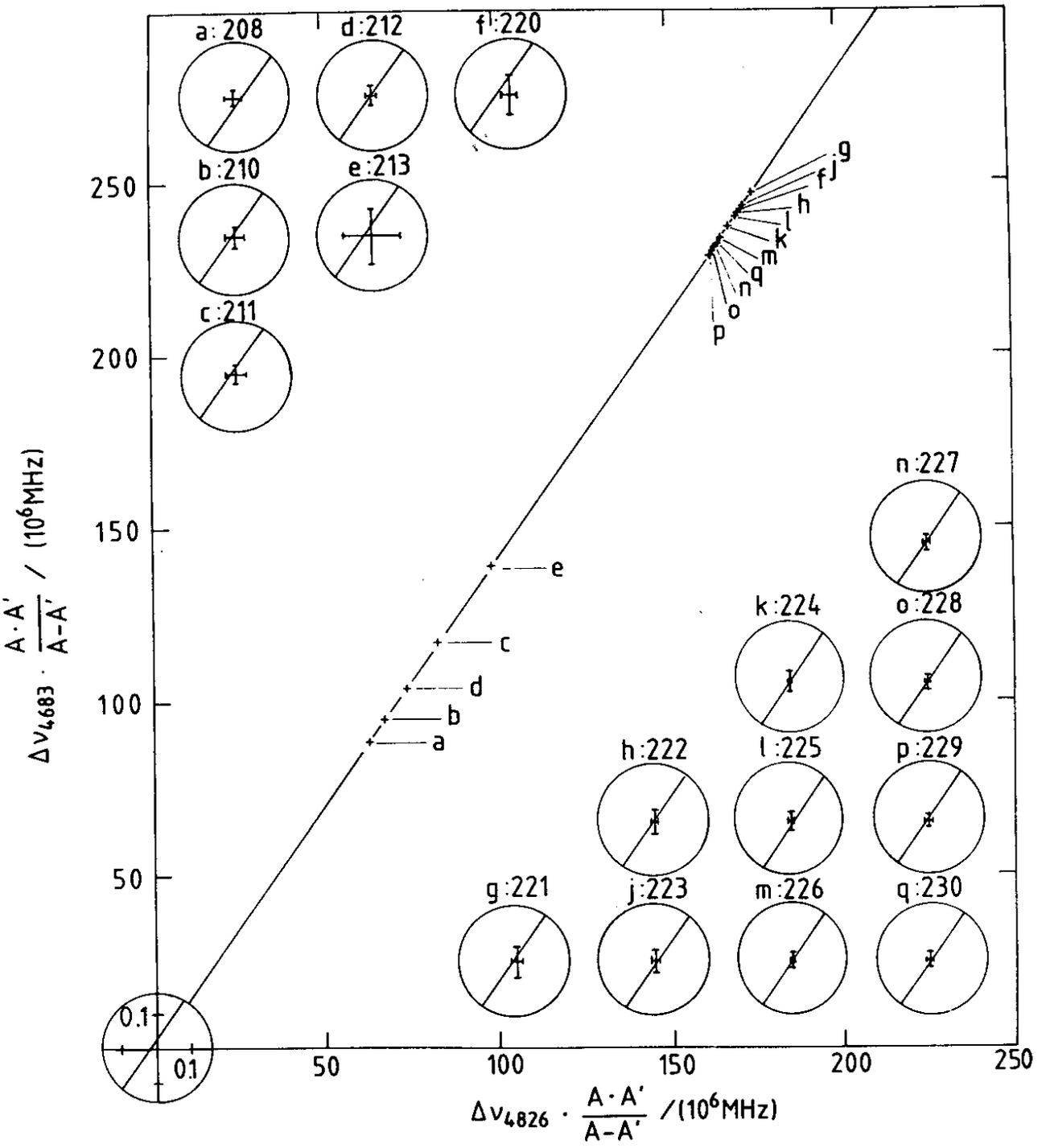
a: 208
d: 212
f: 220
b: 210
e: 213
c: 211
n: 227
k: 224
o: 228
h: 222
l: 225
p: 229
g: 221
j: 223
m: 226
q: 230
a
b
c
d
e
f
g
h
j
k
l
m
n
o
p
0.1
0.1
50
100
150
200
250
50
100
150
200
250
$\Delta\nu_{4683} \cdot \frac{A \cdot A'}{A-A'}$ / (10^6MHz)
$\Delta\nu_{4826} \cdot \frac{A \cdot A'}{A-A'}$ /(10^6MHz)

Fig. 4